IOP Conf. Series: Materials Science and Engineering **355** (2018) 012013 doi:10.1088/1757-899X/355/1/012013

Comparison of Electromagnetic and Marangoni Forces on Thin Coatings during Rapid Heating Process

T Steinberg[1], T Opitz[2], A Rybakov[1], E Baake[1]

[1] Institute of Electrotechnology, Leibniz Universität Hannover, D-30167 Hanover, Germany
[2] Volkswagen AG, D-38440 Wolfsburg, Germany

steinberg@etp.uni-hannover.de

Abstract. The present paper is dedicated to the investigation of Marangoni and Lorentz forces in a rapid heating process. During the melting of aluminum-silicon (AlSi) layer on the bor-manganese steel 22MnB5, the liquid AlSi is shifting from the middle to the side and leaves dry spots on the steel due to a combination of both forces. In order to solve this process design issue, the impact of each force in the process will be evaluated. Evaluation is carried out using experimental data and numerical simulation.

1. Introduction

The passenger car represents the biggest stand-alone consumer of energy as well as CO2 emitter in the European Union. The EU-directive 333/2014, based on 443/2009 has set a goal of CO2 emission reduction of new passenger cars to 95 g CO2/km till 2020 [1–3]. In addition the demand for lightweight construction is strongly increasing due to range extension in electro-mobility [4].
The body in white - with 40 % of total car weight - represents a crucial adjusting screw in order to obtain these goals on time. The manufacturing method of hot forming enables the production of high-strength and complex shaped parts for automotive BIW-construction and therefore reveals a huge potential in lightweight design with over 600 million hot formed parts per year and an increasing usage in future (Fig. 1).

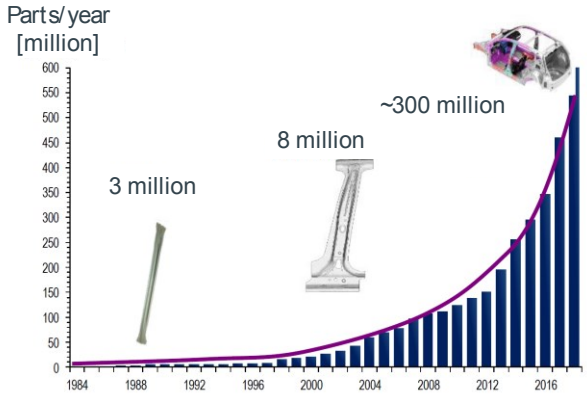

Figure 1. Development and trend of hot forming [5].

During hot forming a boron-manganese steel alloy exhibiting a high hardenability is heated and austenitized at temperatures above 900°C to yield a fully austenitic microstructure. After a dwell time of 4-6 minutes in a gas heated roller hearth furnace (30-40 m) the blank is transferred into a press, where it is quenched and formed simultaneously.
Coating of the blanks with an Al-Si-layer is necessary in order to reduce the wear of hot forming tools due to scale formation in the furnace. Scale in hot forming tools is responsible for up to 40 % of tool wear [6]. In addition the Al-Fe-Si serves as an anti-corrosion barrier in the finished part without downstreamed shot blasting procedure.
The long roller hearth furnaces, long dwell times and high process temperatures lead to a low efficiency of the hot forming process that could be counteracted by the application of e.g. fast heating methods like induction. Using a fast inductive pre-heating to Curie-temperature of the substrate material, the necessary heating time to dwell temperature could be reduced by up to 50 % [7]. The application of fast heating in hot forming is restrained by AlSi-coating melting and dislocation due to large thermic and magnetic forces accompanied by temperature and field density gradients [8].
It remains unclear whether thermal gradients or variations in magnetic pressure are responsible for AlSi-coating dislocation during rapid heating. Therefore the thermal as well as magnetic contributions are simulated, discussed and validated with real experiments to characterize the main driving force.

2. Experiments

Experimental observations of longitudinal inductive rapid heating show a significant wave-shaped coating flow along the melting-zone of AlSi-coated hot forming steel. The temperature distribution inside of the inductor show an outwards orientated decrease in temperature with a maximum in the middle that goes hand in hand with a gradient in the magnetic field density inside of the inductor. Therefore the melting first occurs in the center-region and the flow is directed to out regions exhibiting lower temperatures and lower magnetic pressure. The experiments are conducted with an inductive heating unit shown in Fig. 2, using a capacity of 4 x 330 nF, a current of 68 A and a AC-frequency of 250 kHz. The inductor exhibits six water cooled copper coils with an internal spacing of 20 mm.

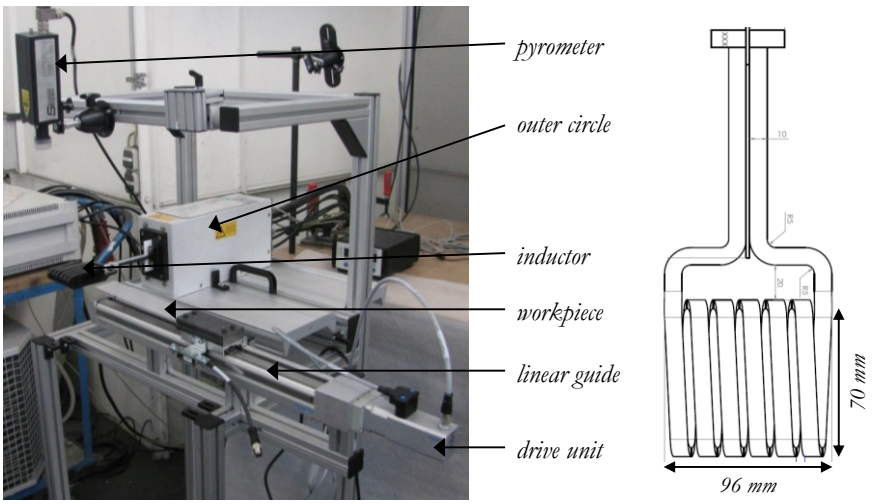

Figure 2. Experimental Setup for inductive heating experiments in dynamic and static mode.

Coated samples with geometry of 250 x 50 x 1.8 mm are inductively heated to temperatures of 700, 800 and 900°C within eight seconds. The workpiece is mounted statically inside the inductor that exhibits coil dimensions of 96 x 70 x 20 mm. The temperature is measured optically by pyrometer after conducting a calibration curve with thermocouples welded onto the material (Fig. 3, left). The highest temperature is obtained directly in the center of the inductor (~ point 2) and the temperature

decreases by approximately 150 K in a 20 mm distance (~ point 4) for the 700°C measurement. Coating melting is initiated in the center after locally overshooting the melting temperature of ~580°C. Afterwards the liquid phase flows to the outer sides that subsequently undergo a phase transition. The coating thickness is measured by metallographic cross section polishes because nondestructive measurements are strongly afflicted by errors due to different intermetallic phases. Hereby the coating thickness is measured from the substrate to the coating surface and includes the intermetallic phase (with higher melting point). The thickness measurement demonstrated in Fig. 3 on the right shows the formation of a minimum/depression in the region of the intermetallic phase thickness between 10 and 14 µm and the formation of a maximum in the outer inductor regions. The coating piles up to a thickness of over 300 µm at the resolidfied wave front.

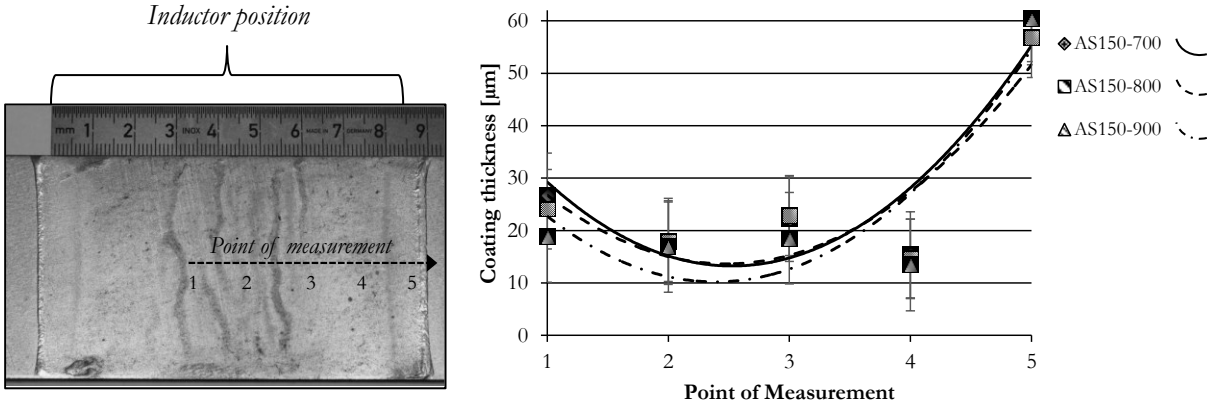

Figure 3. Positions of metallographic thickness measurements (left) and resulting coating thickness after inductive heating of AS150-coated blanks to temp. between 700 and 900°C (right).

The coating development and dislocation is equal for both sides of the blanks, therefore the gravitational effect does not play a crucial role in the phenomenon.

3. Physical model and numerical simulation

To further observe the phenomenon a CFD-Simulation using the VOF-model is built in ANSYS Fluent that only contributes to surface tension related Marangoni as well as gravitational forces. The steel substrate is treated as a non-slip boundary condition with an applied temperature field. Initial phase fraction distribution of AlSi, air and the transition zone of both phases, which results from the VoF-model, is shown in Fig. 4. All material parameters are chosen temperature depended and triangular temperature profile has been used that exhibits the highest temperature in the center of the blank and declines with 7.5 K/mm to the outer side of the blank. To reduce the necessary time for calculation a symmetry condition is used in the middle and only one half of the induction field is observed.

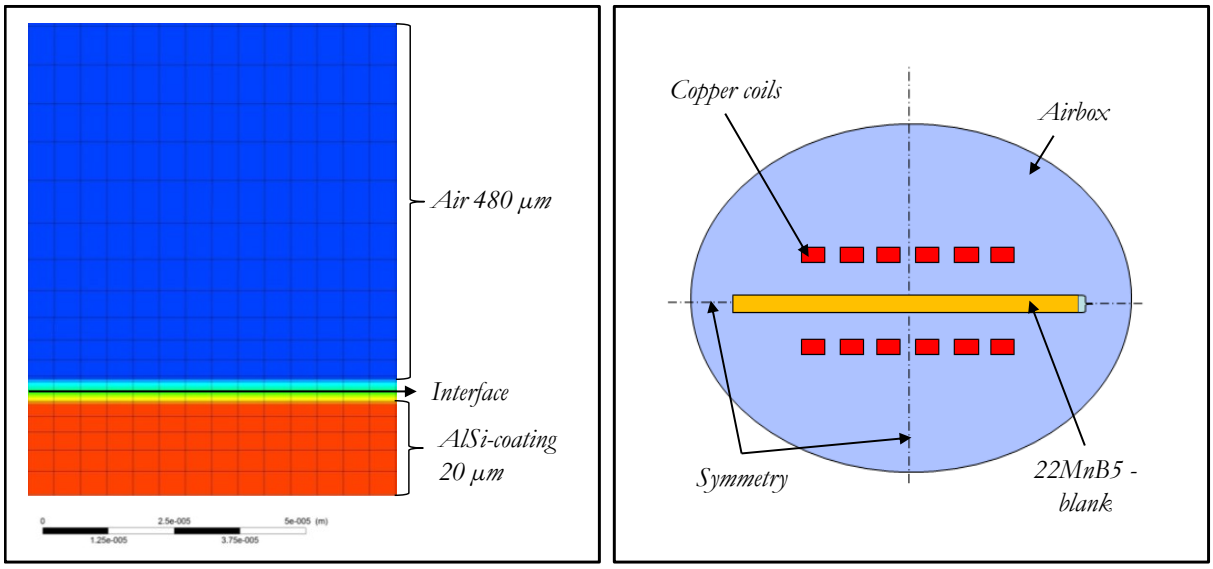

Figure 4. (left) 2D-Replacement model for VOF-Simulation containing mesh information and position of VOF 0.5-interface; (right) sketch of 2D Simulation model for coupled electromagnetic and thermal simulation.

A variable time step is used to account for a correct tracing of the interface by the PLIC-scheme. The melting is simulated with the "ANSYS melting and solidification model". The triangular temperature profile leads to the formation of a dryspot in the center at the point of the highest temperature and a wave formation being upstream of the film delamination. If only the Marangoni force in terms of temperature gradient over the surface is taken into account – a comparable effect to the experiment can be observed in the simulation (Fig. 5).

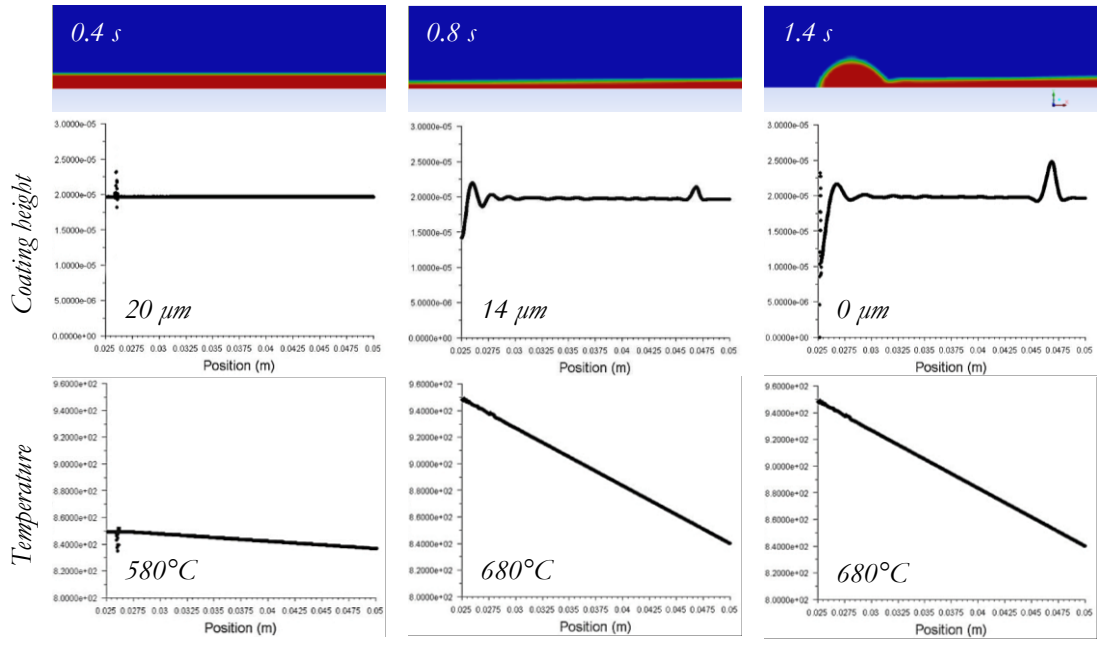

Figure 5. 2D-VOF-simulation sequence from coating melting (t=0.4s) over dryspot formation (t=0.8) till wave propagation (t=1.4s) based on a triangle temperature profile and resulting Marangoni forces by applying a temperature gradient of 70 °C over a measuring length of 50 mm.

The simulations with and without gravitational body forces show a nearly identical result. Therefore gravitation can be neglected.
Lorentzian force on the coating in x-direction due to gradients in magnetic field can be written as follows:

$$\frac{\partial P_{el,m}}{\partial x} = \frac{1}{2}\mu_0(\delta_C + \frac{\delta}{2}\left[1 - e^{\left(-2\frac{\delta_{coating}}{\delta}\right)}\right])\frac{\partial H_{em}^2}{\partial x} \quad (1)$$

where δ represents the pentration depth, μ_0 magnetic field constant and $\frac{\partial H_{em}^2}{\partial x}$ the square of the magnetic field intensity. The numerical expression is yielded based on Lupi et al. [9].
In order to evaluate the impact of Lorentzian forces, a coupled electromagnetic and thermal numerical model is built and simulation is performed by using ANSYS Multiphysics software package. The numerical model is verified by comparing the results with experimental data. The geometry is a planar two-dimensional geometry, which represents the six inductor windings, as well as the manganese steel and the AlSi coating surrounded by an air box. During the experiment electrical parameters such as voltage, current and frequency have been recorded, wherein current and frequency are serving as input parameters for the simulation. Current and frequency has been measured using a Rogowski-belt, which is placed around the inductor and outputs a current proportional voltage with the identical frequency of primary current. The values of current are oscillating around 65 – 70 A RMS. Frequency changes due to temperature dependent material properties from 252 – 217 kHz. Inductor voltage is directly measured at the connections of the inductor by removing electrical insulation coating. The voltage resulting from simulation is used, as well as the temperature, as verification for the validity of the model. The results of thermal calculation are shown in Fig. 6. The non-linear permeability of manganese steel in the simulation is the most crucial material parameter. Dependency of both, temperature and magnetic field intensity has to be taken into account. The difference of the temperature between simulation and experiment is in the range of 6 % or 10 K. The difference of electric voltage in simulation and experiment is around 16 %. Due to the simplification of the model to a 2D geometry and the neglection of the inductor connection results in a lower simulated inductivity and thus to a lower calculated voltage of the inductor. All in all, experimental and numerical results are in a good agreement and magnetic field results will be used for estimation of Lorentzian force.

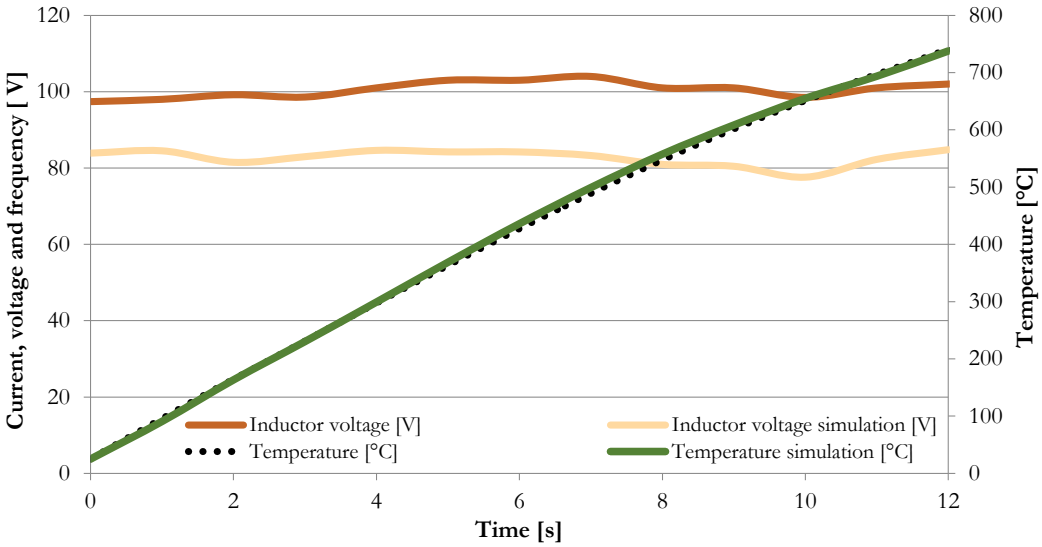

Figure 6. Measured and simulated data validation for electromagnetic force evaluation.

4. Results/Discussion

The schematic drawing in Fig. 7 gives a summary of the investigated phaenomenon. A current carrying inductor winding is located above a AlSi-coated steel substrate, that is inductively heated up due to induced eddy currents. During the heating process the AlSi coating is melted and a motion of the resulting liquid phase from the middle under the inductor to the sides can be observed. Especially in broader regions of the liquid coating, a convective flow with rolling characteristics is expected.

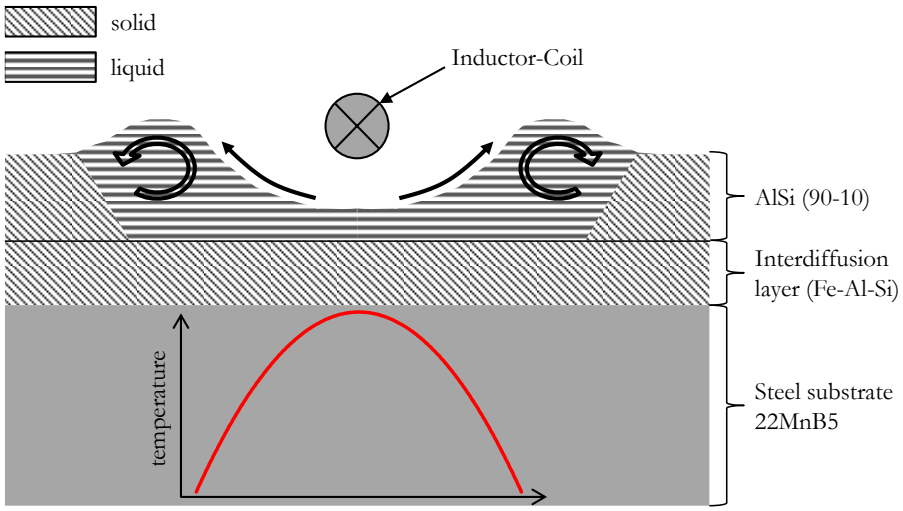

Figure 7. Schematic drawing of AlSi-coating behavior during fast and local heating above melting Temp.

The inductor creates a strong magnetic field intensity, which induces a high energy density inside of the workpiece and results in a temperature distribution with high temperature gradients. Due to these temperature gradients melting occurrence, the Marangoni force acts in the direction from high temperature to low temperature on the liquid phase. A drop in temperature is experimentally measured to approximately 150 – 200 K. Beyond the outer windings of the inductor temperature drops almost to room temperature. Especially from the middle to the outer part of the inductor high temperature gradients are created. This distribution is shown schematically in Fig. 8. According to equation (2) the temperature gradient is the driving force of the Marangoni force and is directed from high temperature to low temperature. As indicated, the equation has the dimension of a pressure. In order to obtain the driving volume force on the melt, the derivation of pressure in x-direction is calculated. σT represents the gradient of the surface tension with the temperature and is a monotonous decreasing function exhibiting a value of -3·10-4 N/mK. The data for the surface tension of AlSi(90-10) are taken out of simulations with the commercial software package JMatPro, using the TTAL8-thermotech database.

$$\frac{\partial F_\sigma}{\partial x} = P_{Marangoni} = -\sigma_T \frac{\partial T}{\partial x} \tag{2}$$

$$\frac{\partial P_{Marangoni}}{\partial x} = -\sigma_T \frac{\partial^2 T}{\partial x^2} \tag{3}$$

According to equation (1) the gradient of the squared magnetic field below the inductor and inside of the AlSi region is calculated and evaluated regarding the resulting force. In figure 8 the gradient of the squared magnetic field intensity is shown in relation to the inductor position. The highest gradient appears at the edges of the outer inductor windings, where the highest changing of potential lines of magnetic field takes place. In this case the maximum gradient is appr. $2*10^9$ [A²/m³], whereas the maximum magnetic field intensity appears in the middle of the inductor. As shown in Fig. 8 the maximum field intensity is appr. 6000 [A/m]. A comparison of the Lorentzian and Marangoni leads to:

$$\frac{\partial F_{el,m}}{\partial x}\Big/\frac{\partial F_\sigma}{\partial x} = \frac{\mu_0\mu_r}{2\sigma_T}\left(\delta_C + \frac{\delta}{2}\left[1 - e^{-2(\frac{\delta_C}{\delta})}\right]\right)\frac{\partial H^2}{\partial x}\Big/\frac{\partial T}{\partial x} \quad (4)$$

including the following material parameters for the liquid phase: σT=3·10-4 [N/mK], penetration depth of the electromagnetic field δ=0.207 [mm], thickness of the AlSi coating δcoating=30 [µm] and relative permeability µr=1. The first part on the left side depends on coating properties only, while the second term depends on the process parameters magnetic field and temperature, which are linked directly to electric current. The first term can be calculated for given material properties and general geometry and results to $1.64*10^{-7}$. Due to small coating surface and the coating dependent properties the Marangoni forces are in this case under the inductor in a range of 20 mm around 130 times higher. Situation is of course changing with temperature equalization and location. Especially at the edges of the inductor, the Lorentzian force becomes higher compared to Marangoni forces.
Both, Marangoni forces and Lorentzian forces point in the direction of less magnetic pressure and lower temperature, which is in this situation the same direction and lead to self-strengthening effect on the coating surface.

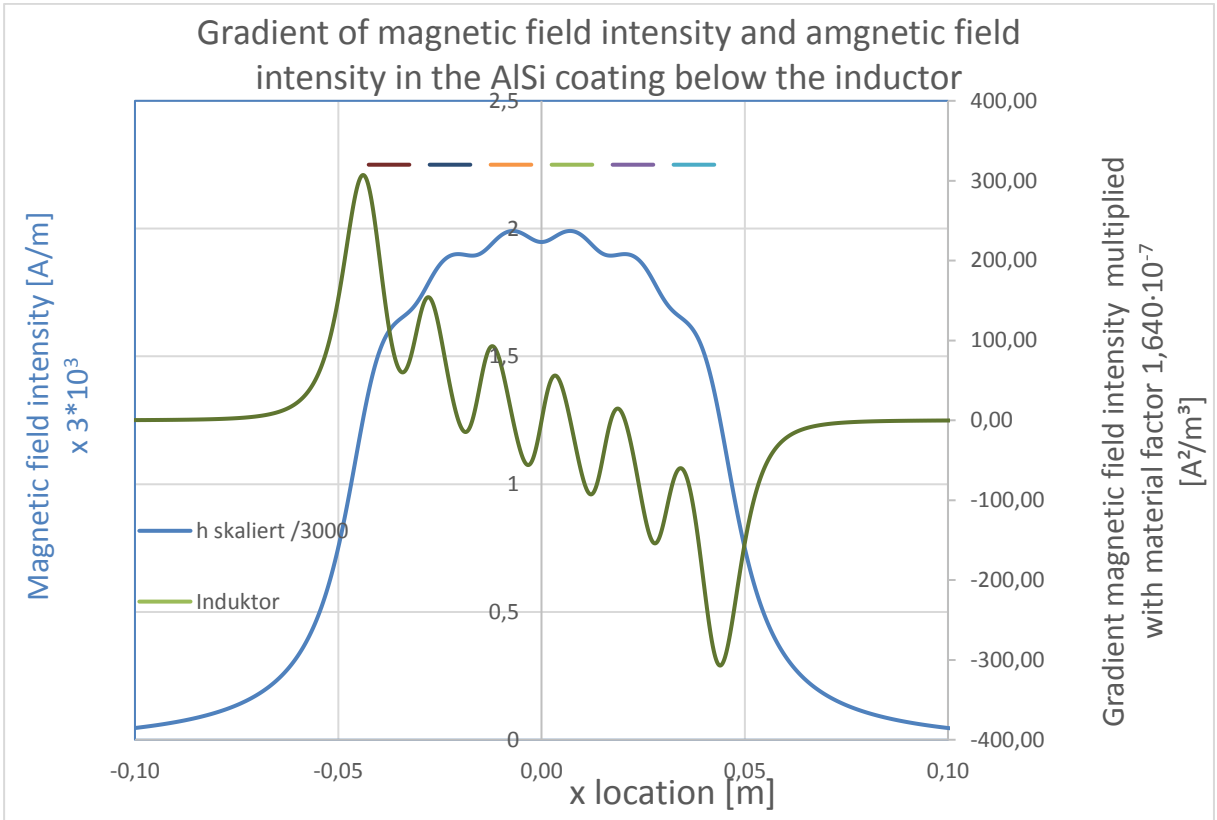

Figure 8. Resulting electromagnetic field intensity and behavior of the spatial derivative representing the electromagnetic force contribution.

5. Conclusion

The contributions of magnetic Lorentzian body forces, temperature and surface tension dependent Marangoni forces as well as gravitational forces are numerically analyzed and weighted for the present case of static inductive heating for hot forming at temperatures above 580 °C. The outcomes can be summarized as follows:

- Lorentzian forces are mainly depending on the spatial derivative of the squared magnetic field strength and pointing as a body force onto the liquid phase in direction from high magnetic to low magnetic pressures. The highest force is obtained at the outer edges of the inductor and decays in the inner areas.
- The Marangoni force is a function of the temperature gradient, acting at the rim of the melting zone. The vector of this surface tension force is congruent to the magnetic force, exhibiting a decreasing contribution in the inner inductor regions due to temperature gradient reduction.
- In summary it can be stated that the Marangoni as well as Lorentzian force contribution are adding up to the net driving force on the liquid phase with an expected higher contribution of the Marangoni forces in the present case, mainly affected by small coating thicknesses of 20-30 μm in hot forming.

Acknowledgement

The authors gratefully acknowledge the informational support of the university department “convective transport processes” of RWTH Aachen.

References

[1] Haq G, Weiss M, 2016 CO2 labelling of passenger cars in Europe: Status, challenges, and future prospects. *Energy Policy* 95, 324–335

[2] Europäisches Parlament, Amt für Veröffentlichungen, Verordnung (EU) Nr. 333/2014 des Europäischen Parlaments und des Rates vom 11. März 2014 zur Änderung der Verordnung (EG) Nr. 443/2009 hinsichtlich der Festlegung der Modalitäten für das Erreichen des Ziels für 2020 zur Verringerung der CO2-Emissionen neuer Personenkraftwagen, 2014

[3] Europäisches Parlament, Amt für Veröffentlichungen, Verordnung (EG) Nr. 443/2009 des Europäischen Parlaments und des Rates vom 23. April 2009 zur Festsetzung von Emissionsnormen für neue Personenkraftwagen im Rahmen des Gesamtkonzepts der Gemeinschaft zur Verringerung der CO2-Emissionen von Personenkraftwagen und leichten Nutzfahrzeugen 2009

[4] Hirsch J, 2016 May 11Approach for an all-aluminium lightweight car body for electric vehicles. *Materials in Car Body Engineering*, Bad Nauheim

[5] Aspacher J, Higher efficiency, output and part quality by newest developments of press technology. Strategien des Karosseriebaus, Bad Nauheim 2016 Mar 15

[6] Sartor M, Khalil T, Schoppe J, September 2012 Verringerung der Zunderbildung durch Beschichtungen. *Schmiedejournal*, 50–52.

[7] Vibrans T, 2016 Entwicklung einer Anlage zur induktiven Erwärmung von Formplatinen. elektrowärme international 2016, 39–44

[8] Opitz T, Induktive Schnellerwärmung von Formplatinen für die Warmumformung im Karosseriebau. HTM J. *Heat Treatent Mat.* 70 2015, 201–206

[9] Lupi S, Forzan M et al, 2015 Induction and direct resistance heating: Theory and numerical modeling, Springer, Cham